JOURNAL OF Materials CHEMISTRY

Synthesis, structure and properties of benzoic acids bearing *para*- or *meta*-imino nitroxides or *ortho*-nitronyl nitroxide radical centres

Christophe Stroh,[a] Francisco M. Romero,[a] Nathalie Kyritsakas,[b] Laure Catala,[c,d] Philippe Turek[d] and Raymond Ziessel*[a]

[a]*Laboratoire de Chimie, d'Electronique et de Photonique Moléculaires, Ecole Chimie, Polymères, Matériaux (ECPM), Université Louis Pasteur (ULP), 25 rue Becquerel, 67087 Strasbourg Cédex 2, France*
[b]*Laboratoire de Cristallochimie et de Chimie Structurale, ULP, Institut le Bel, 4 rue Blaise Pascal, 67008 Strasbourg, France*
[c]*Institut Charles Sadron, ULP, 6 rue Boussingault, 67083 Strasbourg Cédex, France*
[d]*Institut de Physique et Chimie des Matériaux, 23 rue du Loess, BP 20, 67037 Strasbourg Cédex, France*

Received 15th October 1998, Accepted 18th December 1998

2-(4-Carboxyphenyl)-4,4,5,5-tetramethyl-4,5-dihydro-1*H*-imidazol-1-yloxyl (*p*-IMBAH), 2-(3-carboxyphenyl)-4,4,5,5-tetramethyl-4,5-dihydro-1*H*-imidazol-1-yloxyl (*m*-IMBAH) and 2-(2-carboxyphenyl)-4,4,5,5-tetramethyl-4,5-dihydro-3-oxido-1*H*-imidazol-3-ium-1-yloxyl (*o*-NITBAH) have been prepared. The *m*-IMBAH and *p*-IMBAH radicals crystallised in monoclinic space group $P2_1/n$ while the *o*-NITBAH radical occupied the monoclinic space group *Cc*. In *p*-IMBAH, a 12-membered ring is formed *via* strong hydrogen bonds between two water molecules and two radicals, this unit being propagated along the *b* axis *via* additional hydrogen bonds. In *m*-IMBAH, the radicals are arranged in dimers held together by strong hydrogen bonds between the acid and the imine functions, each dimer being connected with its neighbours *via* hydrogen bonds forming alternating chains along the *c* axis. No cyclic arrangements are evident in *o*-NITBAH, the radicals being organized into infinite chains. In each case, the product of paramagnetic susceptibility with *T* lies in the 0.362 to 0.374 emu K mol^{-1} range at room temperature while the reciprocal susceptibility follows a Curie–Weiss law above 20 K with $\theta = +1.38$, $+5.24$ and -0.81 K, respectively, for *p*-IMBAH, *m*-IMBAH and *o*-NITBAH. The isotropic ^{14}N hyperfine coupling constants are found from solution experiments to be 9.20 (a_{N1}) and 4.28 (a_{N2}) G for the imino radicals and 7.59 G for the nitronyl nitroxide radical. The principal values of the *g*-tensor measured on single crystals afforded an average of 2.0066/7 while in solution $g_{iso} = 2.0060$ for *p*/*m*-IMBAH and 2.0065 for *o*-NITBAH.

A considerable challenge facing the field of material science concerns the search for novel spin systems displaying valuable physical properties such as high T_c ferro- or ferrimagnets.[1] Substantial progress has been made since the discovery of the first purely organic ferromagnets.[2–4] However, the ordering temperature remains too low, mostly because of unfavourable orientation of the spins and poor control of the dimensionality of the material. A way to control the relative orientation of open-shell molecules is to employ directed hydrogen bonds to organise the solid-state structure. This approach has currently been much used in the field of crystal engineering.[5] Transmission of magnetic interactions through hydrogen bonds was first observed with transition metal complexes,[6] but hydrogen-bonded organic ferromagnets have now been reported with hydroquinone[7] or hydroxyphenyl[8] subunits.

We have recently reported that acetylenic hydrogen bonds can be used for the construction of magnetically coupled structures.[9] In fact, according to polarized neutron diffraction studies, a significant spin density is present on the hydrogen-bonding site with a concomitant depletion of the spin density of the nitroxide involved in the hydrogen bond.[10] However, despite clarifying the role played by the hydrogen-bonding site involved in transmitting the spin-polarization it has not been possible to accurately predict the dimensionality of the magnetic interaction in such systems.[11]

The potentiality that nitronyl nitroxides (NIT) or imino nitroxides (IM) carrying carboxylic or sulfonic acid functions allow preparation of multi-dimensional magnetic materials prompted us to prepare *ortho*, *meta*, and *para*-benzoic acids bearing nitroxide fragments. The coordination chemistry and magnetic behaviour of *para*-NIT-benzoic acid were previously investigated,[12,13] while carboxylic acid radicals have been used to prepare supramolecular multi-layered materials that exhibit a hysteresis loop characteristic of ferromagnetic-like three dimensional order.[14,15] Nitronyl nitroxide substituted carboxylic acids or their alkali metal salts have been used widely as spin labels or as antidotes (for nitric oxide) in pharmacology.[16–18] Surprisingly, IM-benzoic acids substituted in the *meta*-position and NIT-benzoic acids functionalized at the *ortho*-position have not been isolated to date. The preparation of *para*-IM-benzoic acid has been mentioned[19] briefly in the literature but its characterization, including electronic and magnetic properties, has not been documented.

We now report full synthetic data, X-ray structural studies and electronic and magnetic properties for *para*-IM-benzoic acid (*p*-IMBAH), *meta*-IM-benzoic acid (*m*-IMBAH), and *ortho*-NIT-benzoic acid (*o*-NITBAH).

Results and discussion

Synthesis

Benzoic acids-based nitroxide monoradicals were prepared in good yield according to a general method reported previously[20] that involves condensation of *N*,*N*′-dihydroxy-2,3-diamino-2,3-dimethylbutane[21] with the commercially-available aldehydes in methanol as outlined in Scheme 1.

Mild oxidation of the crude material using phase transfer conditions in a mixture of dichloromethane–water and sodium periodate as oxidant afforded the orange–red *para*- and *meta*-imino nitroxides. Condensation at room-temperature of

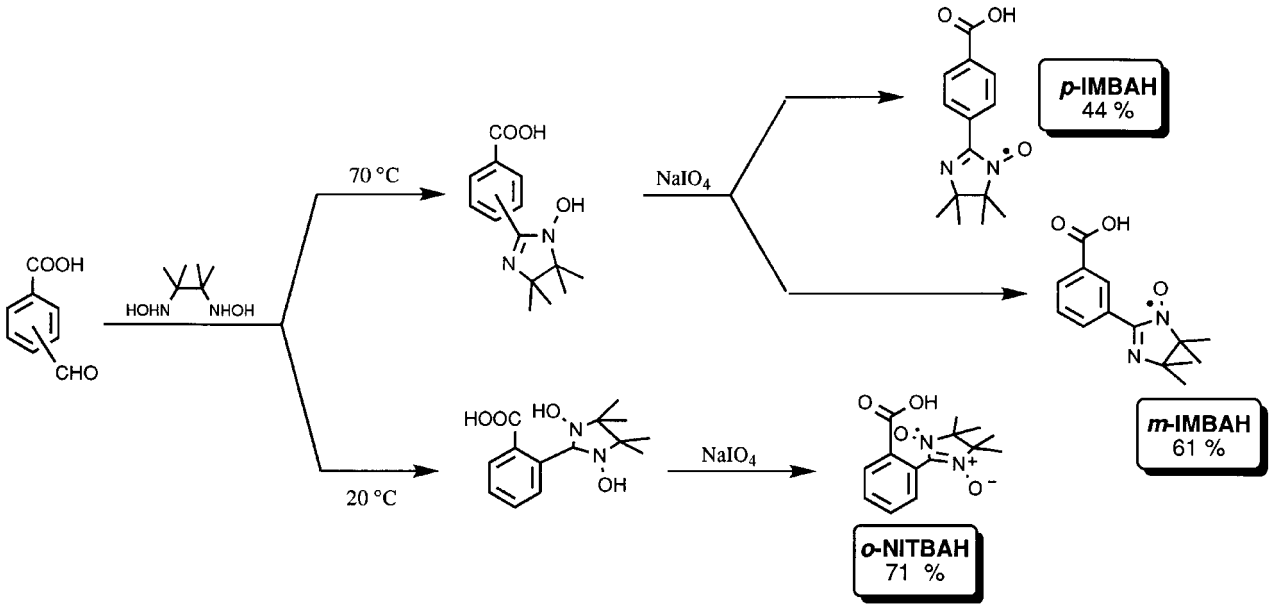

Scheme 1

o-carboxybenzaldehyde affords the dihydroxyimidazolidine intermediate which, after oxidation under the same conditions, gives the stable deep-violet nitronyl nitroxide radical. All three radicals were characterized by X-ray diffraction, FT-IR, UV–VIS, EPR, magnetic measurements and by elemental analysis. Selected data are gathered in Table 1.

Crystal structure

Single crystals of *p*-IMBAH and *o*-NITBAH were grown from a mixture of dichloromethane–hexane and chloroform–hexane respectively, while crystals of *m*-IMBAH were obtained by slow diffusion of pentane in a diethyl ether solution.

***p*-IMBAH.** In the molecular structure of the *para*-isomer the benzene ring is tilted with respect to the imino radical by an angle of *ca.* 19° and relative to the carboxylic function by *ca.* 2° [Fig. 1(a)]. A water molecule is surrounded at hydrogen bond contact distance by the imine function of one radical [N(2)···H(19) 1.90 Å], by the acid hydroxy function of a second radical [H′(17)···O(w) 1.51 Å], and by the acid carbonyl function of a third radical [O″(2)···H(18) 1.87 Å] as shown in Fig. 1(b). Relevant angles around the water molecule are N(2)···H(19)–O(w) 166.6°, O′(1)–H′(17)···O(w) 170.2°, O″(2)···H(18)–O(w) 163.5°. This special arrangement is propagated along the *b* axis, giving the appearance of an extended chain, as shown in Fig. 2. The shortest interchain distance involving the N–O unit is 2.78 Å [O(3)···H‴C‴(2)] and the shortest radical–radical distance is 4.75 Å [O(3)···N‴(2)], both along the *c* direction. This crystal structure differs markedly from that of the *p*-NITBAH where the packing arrrangement shows no water molecules and the radicals are connected in pairs of one-dimensional chain structures with a single hydrogen bond between the carboxylic acid group and the nitronyl nitroxide oxygen.[13]

***m*-IMBAH.** In the molecular structure of the *meta*-isomer the radical is tilted by *ca.* 26° with respect to the phenyl ring and *ca.* 8° with the carboxylic fragment [Fig. 3(a)]. Adjacent radicals are organised in a head-to-tail fashion to form dimers with strong hydrogen bonds between acid and imine of the radical [N(2)···H′(17) 1.82 Å]. The net result is a giant 16-membered void as shown in Fig. 3(b). Each dimer is connected along the *c* axis *via* contacts between the N–O and a proton at the *para* position *versus* the carboxylic function, to form alternating chains [O(1)···H″C″(9) 2.79 Å] as shown in Fig. 4. The shortest interdimer radical-radical distance related by an inversion center is 4.03 Å [O(1)···O′(1)] while the shortest interchain distance involves only protons on the methyl groups.

***o*-NITBAH.** In the molecular structure of the *ortho* compound, the nitronyl nitroxide radical and the carboxylic unit respectively are tilted by *ca.* 75 and 21° with the phenyl ring [Fig. 5(a)]. In this structure, the position of the carboxylic proton could not be located precisely. The intramolecular distance between the acid function and the NO fragment of one radical is 3.39 Å [O(3)···O(2)]. The radicals are organised into chains by strong hydrogen bonds between O(1)···O(7) (2.59 Å) and O(5)···O′(4) (2.58 Å) as shown in Fig. 5(b). The

Table 1 Selected analytical data for the benzoic acid radicals

Compounds	Isolated yields (%)	IR[a] ν/ cm^{-1}	UV–VIS[b] λ_{max}/ nm (ε/$M^{-1}\,cm^{-1}$)	μ_B (290 K)	Elemental C,H,N analysis (calc.)
p-IMBAH	44	1694	448 (360)	1.727	59.91 (60.20)
		1578			6.77 (6.86)
		1310			10.09 (10.03)[c]
m-IMBAH	61	1695	448 (354)	1.704	64.28 (64.35)
		1578			6.39 (6.56)
		1310			10.66 (10.72)
o-NITBAH	71	1705	551 (879)	1.733	60.48 (60.64)
		1584			6.02 (6.18)
		1346			10.05 (10.10)

[a]Measured in KBr pellets, stretching vibrations correspond to the acid (1694–1705 cm^{-1} range), to the imine (1578–1584 cm^{-1} range) and to the NO bonds (1310–1346 cm^{-1} range). [b]Measured in dichloromethane. [c]Calculated with one water molecule.

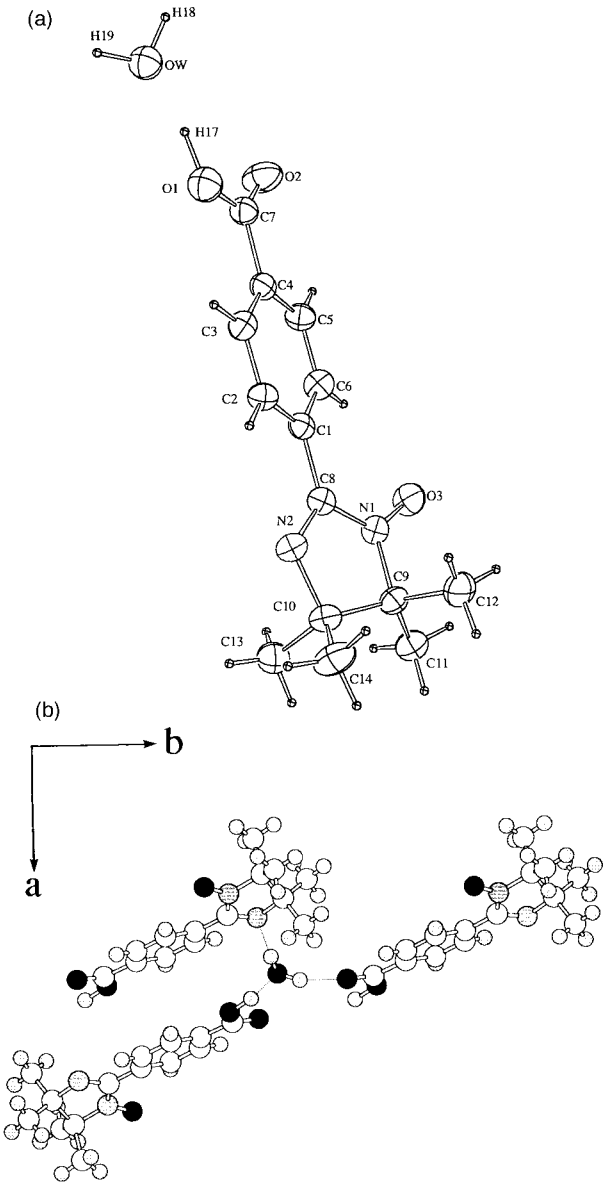

Fig. 1 (a) ORTEP view of a molecular unit of *p*-IMBAH with atom labelling, ellipsoids are scaled to enclose 30% of the electronic density; (b) projection onto the *ab* plane of hydrogen bonds around the water molecule.

shortest interchain distances involve the NO function of one radical and a H-atom belonging to the phenyl group of a neighbouring molecule: [O(1)···H″C″(11) 2.50 Å] and [O(2)···H‴C‴(26) 2.54 Å]. The shortest interchain NO distance is 4.82 Å while the shortest intrachain is 5.86 Å.

For all three radicals, the intramolecular distances and

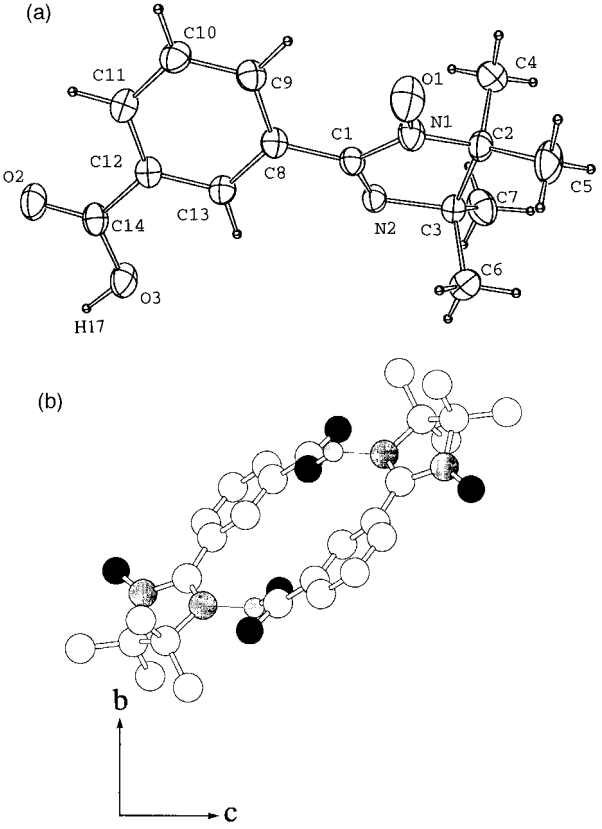

Fig. 3 (a) ORTEP view of a molecular unit of *m*-IMBAH with atom labelling, ellipsoids are scaled to enclose 30% of the electronic density; (b) projection onto the *bc* plane of the dimer.

angles lie in the range expected for imino nitroxide or nitronyl nitroxide radicals and benzoic acid fragments.[9] Important interatomic distances are given in Table 2.

Magnetic and electronic properties

The paramagnetic susceptibilities of microcrystalline samples of the various radicals were measured between 2 and 300 K at a constant field of 0.5 T with the help of a SQUID susceptometer. The temperature dependence of the molar paramagnetic susceptibility χ was obtained and is presented in Fig. 6 in the form of χT *vs.* T plots. At 290 K, χT values of 0.372, 0.362, and 0.374 emu K mol^{-1}, respectively, were obtained for the *p*-IMBAH, *m*-IMBAH, and *o*-NITBAH radicals. These values are close to the theoretical value (0.375 emu K mol^{-1}) calculated for a single $S=1/2$ free radical. The reciprocal susceptibility of the three compounds follows a Curie–Weiss law above 20 K with $\theta=+1.38$, $+5.24$ and -0.81 K respectively for *p*-IMBAH, *m*-IMBAH and *o*-NITBAH. A close examination of the temperature dependence

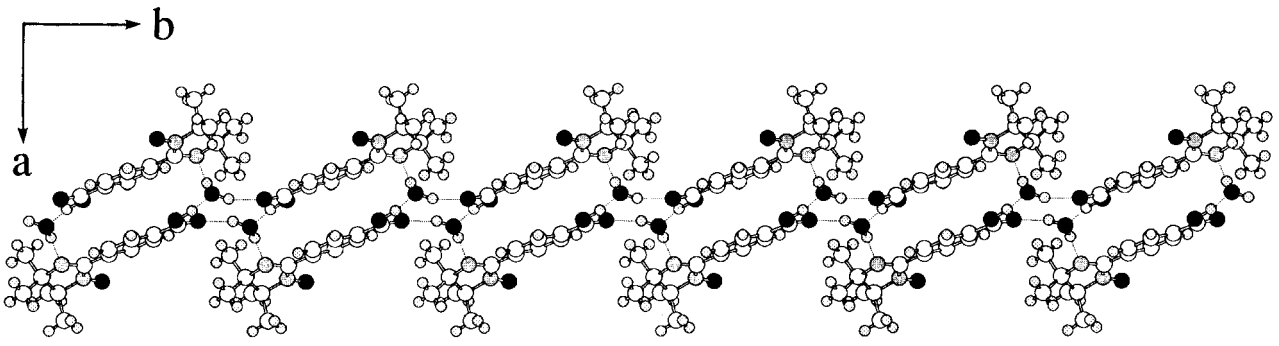

Fig. 2 Projection onto the *ab* plane of the crystal packing of *p*-IMBAH showing the chains running along the *b* direction.

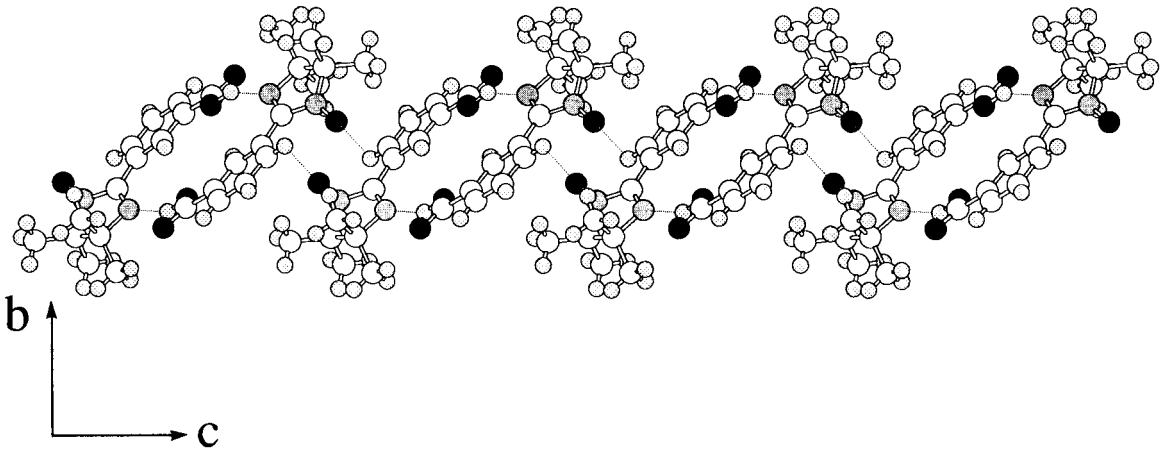

Fig. 4 Projection onto the *bc* plane of the crystal packing of *m*-IMBAH showing the chains running along the *c* direction.

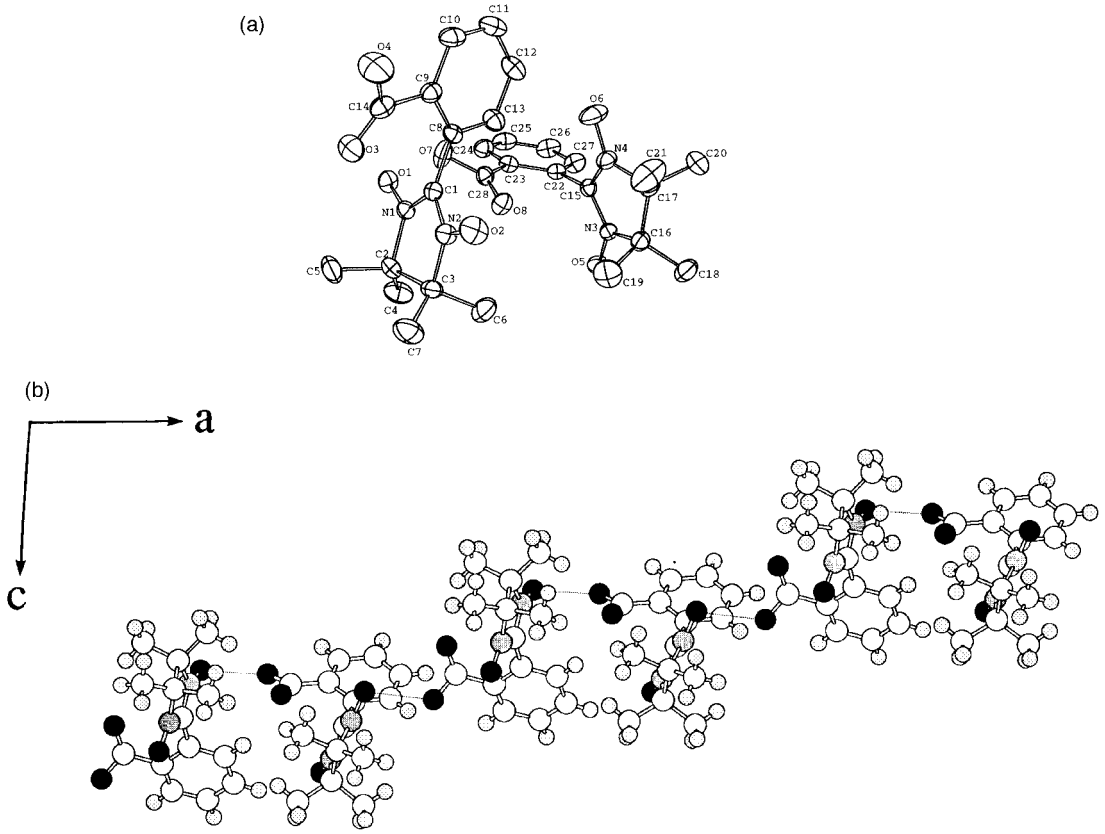

Fig. 5 (a) ORTEP view of a molecular unit of *o*-NITBAH with atom labelling, ellipsoids are scaled to enclose 30% of the electronic density; (b) projection onto the *ac* plane of the crystal packing showing the chains running along the (110) direction.

Table 2 Important interatomic distances (Å) for the three radicals

p-IMBAH		*m*-IMBAH		*o*-NITBAH	
C(8)–N(1)	1.387(4)	C(1)–N(1)	1.404(3)	C(1)–N(1)	1.317(4)
C(8)–N(2)	1.291(4)	C(1)–N(2)	1.288(3)	C(1)–N(2)	1.347(4)
N(1)–O(3)	1.272(3)	N(1)–O(1)	1.264(3)	N(1)–O(1)	1.300(3)
C(7)–O(1)	1.307(4)	C(14)–O(2)	1.202(3)	N(2)–O(2)	1.274(3)
C(7)–O(2)	1.203(4)	C(14)–O(3)	1.325(3)	C(14)–O(3)	1.195(4)
O(1)–H(17)	1.077(4)	O(3)–H(17)	1.005(3)	C(14)–O(4)	1.325(4)
				C(15)–N(3)	1.324(4)
				C(15)–N(4)	1.346(4)
				N(3)–O(5)	1.299(3)
				N(4)–O(6)	1.276(4)
				C(28)–O(7)	1.319(4)
				C(28)–O(8)	1.207(4)

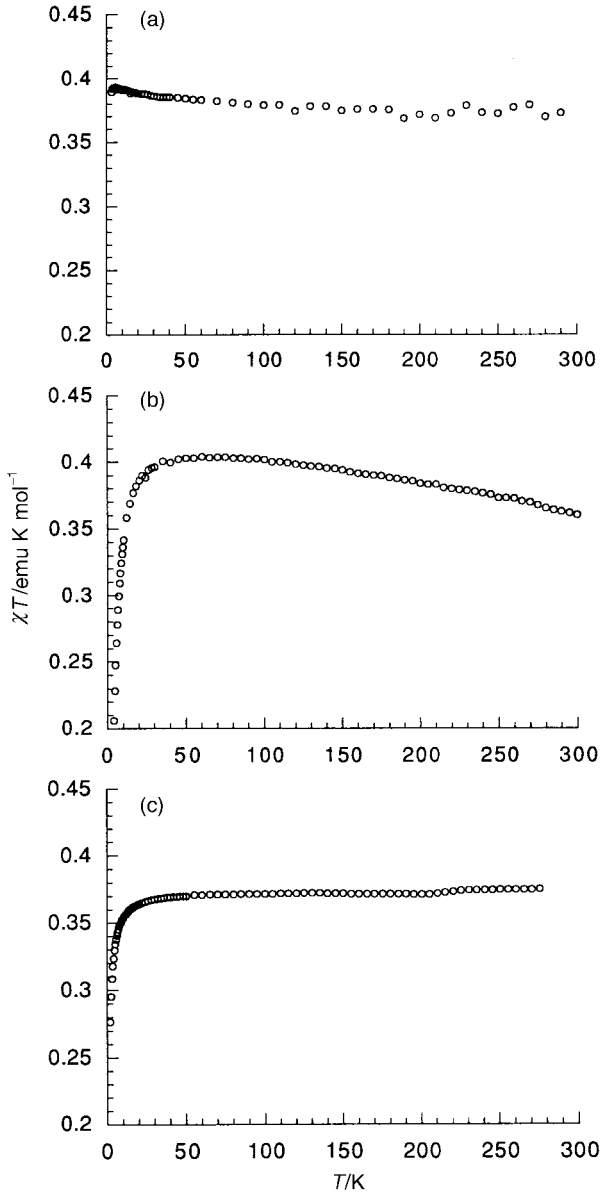

Fig. 6 Temperature dependence of χT for *p*-IMBAH (a), *m*-IMBAH (b) and *o*-NITBAH (c).

of the χT product for the *p*-IMBAH and *m*-IMBAH radicals shows that there is indeed a weak increase between room temperature and *ca.* 20 K, which explains the positive mean-field temperatures derived from Curie–Weiss analysis of the reciprocal susceptibility. However, no satisfactory model (*e.g.* low-dimensional magnetic systems (chains) with mean-field corrections for the interchain magnetic interactions) could be representative of the overall temperature dependence. Both *m*-IMBAH and *o*-NITBAH radicals exhibit downward curvature of the χT product below 20 K which is attributed to weak antiferromagnetic interactions. Based on our analysis of the crystal packing of *p*-IMBAH, the radicals are isolated from near neighbours by the water molecule, giving rise to extremely weak magnetic interactions [Fig. 6(a)]. For *m*-IMBAH, the above analysis of the crystal structure (Fig. 4) suggests the existence of crystallographic chains where the NO groups lie at relatively long distances (>4 Å) with an unfavourable orientation for π-orbital overlap. As such, the magnitude of the magnetic interaction would be weak and, therefore, in accordance with that experimentally observed.

The EPR spectra of the three radicals were recorded at room temperature for diluted and degassed solutions (5×10^{-4} M in CH_2Cl_2) and for single crystals. The hyperfine pattern observed for the molecules in solution was in agreement with the expected sequence for such nitroxide based radicals: i) a seven line EPR spectrum for the imino derivatives due to the hyperfine interaction with two nonequivalent ^{14}N nuclei (N1, N2 in Table 3), and ii) a five line spectrum for *o*-NITBAH (Fig. 7) with two equivalent ^{14}N nuclei. The isotropic ^{14}N hyperfine coupling constants (a_N) and *g*-factors (g_{iso}) were estimated from the simulated hyperfine structure in agreement with the observed pattern (Table 3). They are in keeping with the reported values for such radicals.[22,23] In the solid state, a single exchange-narrowed Lorentzian line was observed at each orientation of the single crystals with respect to the static magnetic field. The principal values of the *g*-tensor were deduced (Table 3) from the rotations of the single crystals around three orthogonal axes. These values are determined by the average orientation of the *g*-tensor of the magnetically nonequivalent molecules within the crystals.[24] However, the lack of knowledge of crystal axes did not allow determination of the principal directions of the *g*-tensor. The average value of the *g*-factor deduced from the principal values of the *g*-tensor (g_{av}) is in good agreement with g_{iso} for *o*-NITBAH. It is interesting to note the differences between g_{iso} and g_{av} for *p*-IMBAH and *m*-IMBAH radicals. Whereas the values of g_{iso} correspond to previously reported values for imino nitroxide radical derivatives, the values of g_{av} are closer to the average values of the *g*-factor of nitronyl nitroxide derivatives.[22] This must be attributed to modification of the spin density distribution over the molecules because of the above described hydrogen bonds. Such effects were demonstrated earlier on a related nitronyl nitroxide compound by polarized neutron diffraction experiments.[10] It follows from previous reports[7–9,23] on the role of the hydrogen bonds in the transmission of the magnetic interactions that a residual spin density over the hydrogen atoms may induce an indirect exchange interaction, although very weak, mediated through

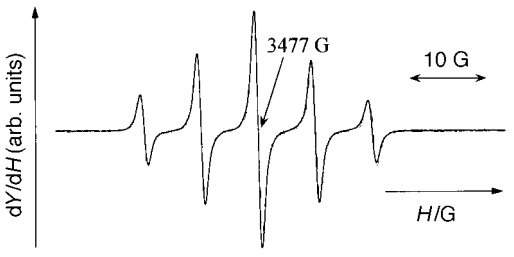

Fig. 7 EPR Spectrum recorded at room temperature for *o*-NITBAH into solution (5×10^{-4} M in CH_2Cl_2). The simulated spectrum ($g=2.0065_6$, $a_N=7.59$ G, individual line width 0.8 lorentzian/gaussian shape: $\Delta B=1.18$ G) is superimposed on the experimental spectrum.

Table 3 Selected EPR data for the benzoic acid radicals[a]

Compound	g_1	g_2	g_3	g_{av}	g_{iso}	a_{N1}/G	a_{N2}/G
p-IMBAH	2.0087_8	2.0075_3	2.0035_2	2.0066_1	2.0060_0	9.20	4.28
m-IMBAH	2.0097_9	2.0054_4	2.0046_5	2.0066_2	2.0060_0	9.20	4.28
o-NITBAH	2.0092_0	2.0082_8	2.0028_9	2.0067_9	2.0065_6	7.59	—

[a]Principal values of the *g*-tensor (g_1, g_2, g_3) as stacked within single crystals and *g*-factor with ^{14}N hyperfine coupling constants for the molecules into degassed dichloromethane solution (g_{iso}, a_N).

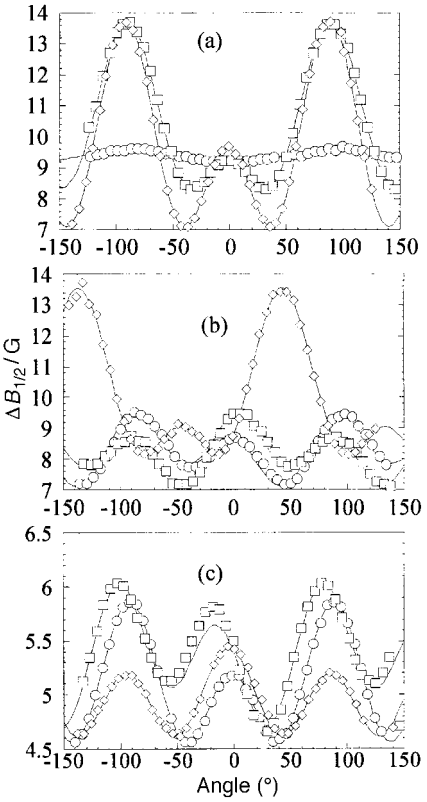

Fig. 8 Angular dependence of the half-width at half maximum of the EPR absorption spectra recorded at room temperature within three orthogonal planes: (a) *p*-IMBAH; (b) *m*-IMBAH; (c) *o*-NITBAH. The continuous lines correspond to the fits of the experimental data with dipolar like trigonometric functions including the squares of the secular ($3\cos^2\theta-1$) and non secular contributions ($\sin\theta\cos\theta$ and $\sin^2\theta$).[25]

the N(imine)···H bonds among the molecular aggregates. This is believed to be at the origin of the observed magnetic behaviour of the IMBAH derivatives. The ^{14}N hyperfine coupling constants (*hfcc*'s) are in agreement with the reported values for such radicals.[24]

The angular dependence of the half-width at half maximum of the absorption spectra, $\Delta B_{1/2}$, has been recorded at room temperature in three orthogonal planes for the single crystals (Fig. 8). The similar values of the extrema of $\Delta B_{1/2}$ for the IMBAH derivatives [Fig. 8(a,b)] express the closely related molecular packings, hence the similar dipolar fields. A peculiar 'W-shape' is observed for the line width anisotropy within some planes. It points to the important weight of the secular dipolar contribution ($3\cos^2\theta-1$) resulting in a minimum of the line width at the magic angle ($\theta\cong54°$), as discussed in the context of the EPR of low-dimensional magnets.[25] However, the reported static magnetic properties and the crystal structure do not allow the unambiguous relation of such a behavior to some low-dimensional spin dynamics, *e.g.* magnetic chains. It is considered that the continuous lines in Fig. 8 are geometrical fits.

Conclusion

The synthesis of *para*- and *meta*-IM-benzoic acid and of *ortho*-NIT-benzoic acid has been achieved and each compound has been properly characterized. The crystal structures of all three stable radicals show significant hydrogen bonding. The magnetic properties of the three compounds can be qualitatively understood in terms of the hydrogen bond being involved in intermolecular magnetic interactions. Modification of the spin density distribution over the molecules is detected through variations of the EPR *g*-tensor. It is attributed to the hydrogen bond formation in the solid, as compared to the isolated molecule probed in solution. The use of strong hydrogen bonds between radicals, carboxylic functions, and water (*p*-IMBAH case) is a good way to organize materials into multidimensional arrays but isolates the spin carriers to such an extent that only dramatically weak magnetic interactions result. It is anticipated that coordination of these radicals to paramagnetic metal centres will avoid formation of these exotic arrangements and will offer new opportunities to prepare hybrid metallo-radical scaffoldings. In spite of the weak magnetic interactions found in these mono-carboxylic acid radicals, crystals of other persistent radicals which are multi-functionalized (*e.g.* dicarboxylic or disulfonic or diphosphonic acids) are suggested to be worthy of further scrutiny for finding significant magnetic interactions among supramolecular acid–base networks.[26]

Experimental

Synthesis

2-(4-Carboxyphenyl)-4,4,5,5-tetramethyl-4,5-dihydro-1*H*-imidazol-1-yloxyl (*p*-IMBAH). A methanol solution (250 ml) of *p*-carboxybenzaldehyde (6.75 g, 45.0 mmol) and *N*,*N*′-dihydroxy-2,3-diamino-2,3-dimethylbutane (6.67 g, 45.0 mmol) was stirred for one day at room temperature before being heated under reflux for 24 h. The yellow precipitate was filtered, washed with methanol, and dried under vacuum to give the monohydroxyimidazolidine (5.66 g, 48% yield). This intermediate was dispersed in dichloromethane (250 ml) and oxidised with an aqueous solution (200 ml) of $NaIO_4$ (8.16 g, 38.2 mmol). After complete disappearance of the suspension (3 hours), the organic phase was separated, extracted with water and dried over $MgSO_4$. The solvent was evaporated under vacuum and the residue purified by flash chromatography on silica (AcOEt–*n*-hexane 1:1). The analytically pure *p*-IMBAH·H_2O radical was obtained as deep-orange crystals by recrystallisation from a mixture of dichloromethane and hexane (5.55 g, 92% yield). Mp 173–174 °C (decomp.). FAB^+ MS *m*/*z* 263.2 $[M+2H+e]^+$. UV–VIS λ_{max}/nm (ε/M^{-1} cm^{-1}) 244 (21429), 302 (3799), 312 (4073), 428 (350), 448 (360). IR (ν/cm^{-1}) 3451, 3211, 2979, 1694 (COOH), 1578 (C=N), 1404, 1375, 1310 (NO), 1265, 1137, 1016, 705 (Found: C, 59.91; H, 6.77; N, 10.09. Calc. for $C_{14}H_{17}N_2O_3\cdot H_2O$ (M_r = 261.303 + 18.015): C, 60.20; H, 6.86; N, 10.03%).

2-(3-Carboxyphenyl)-4,4,5,5-tetramethyl-4,5-dihydro-1*H*-imidazol-1-yloxyl (*m*-IMBAH). *m*-Carboxybenzaldehyde (0.6 g, 4.0 mmol) and *N*,*N*′-dihydroxy-2,3-diamino-2,3-dimethylbutane (0.6 g, 4.1 mmol) were stirred in methanol (25 ml) at room temp. After 3 days, the white suspension was refluxed for 1 hour. The resultant solution was evaporated to dryness. The residue was dissolved in dichloromethane (100 ml) and subsequently oxidized with an aqueous solution (75 ml) of $NaIO_4$ (0.855 g, 4.0 mmol). After 3 hours, the organic phase was separated, extracted with water, and dried over $MgSO_4$. The product was purified by flash chromatography on silica (CH_2Cl_2–MeOH 9:1) to yield, after recrystallization from a mixture of diethyl ether–pentane, deep-orange crystals of *m*-IMBAH (0.64 g, 61% overall yield). Mp 166–167 °C (decomp.). FAB^+ MS *m*/*z* 263.5 $[M+2H+e]^+$. UV–VIS λ/$_{max}$, nm (ε/M^{-1} cm^{-1}) 218 (8209), 244 (19288), 301 (3504), 312 (3734), 429 (340), 448 (354). IR (ν/cm^{-1}) 3450, 3216, 2979, 1695 (COOH), 1578 (C=N), 1450, 1404, 1375, 1130 (NO), 1137, 1105, 864, 798, 779, 705 (Found: C, 64.28; H, 6.39; N, 10.66. Calc. for $C_{14}H_{17}N_2O_3$ (M_r = 261.303): C, 64.35; H, 6.56; N, 10.72%).

2-(2-Carboxyphenyl)-4,4,5,5-tetramethyl-4,5-dihydro-3-oxido-1*H*-imidazol-3-ium-1-yloxyl (*o*-NITBAH). *o*-Carboxy-

Table 4 Crystal data for the three radicals

	p-IMBAH	*m*-IMBAH	*o*-NITBAH
Formula	$C_{14}H_{17}N_2O_3{\cdot}H_2O$	$C_{14}H_{17}N_2O_3$	$C_{14}H_{17}N_2O_4$
MW/g mol^{-1}	279.3	263.3	277.3
Crystal system	Monoclinic	Monoclinic	Monoclinic
Space group	$P2_1/n$	$P2_1/n$	Cc
Lattice parameters	$a=20.403$ (6) Å	$a=6.916$ (2) Å	$a=25.458$ (2) Å
	$b=10.402$ (3) Å	$b=20.003$ (6) Å	$b=7.6775$ (6) Å
	$c=6.824$ (2) Å	$c=10.165$ (3) Å	$c=15.1702$ (5) Å
	$\beta=96.69$ (2)°	$\beta=106.68$ (2)°	$\beta=107.158$ (4)°
Unit cell volume/Å^3	1438.4	1347.1	2833.2
Formula units per cell	4	4	8
Temp. of data coll./°C	−100	20	21
μ/mm^{-1}	0.788	0.092	0.096
Number of data collected	1850	3268	3215
No. of data with $I>3\sigma(I)$	1342	1361	2158
R (F)	0.039	0.043	0.035
Rw (F)	0.058	0.055	0.046

benzaldehyde (0.55 g, 3.7 mmol) and *N*,*N*′-dihydroxy-2,3-diamino-2,3-dimethylbutane (0.55 g, 3.7 mmol) were dissolved in methanol (10 ml) and stirred in the dark at room temp. The formation of a white precipitate was observed after 2 minutes. After 24 hours stirring the dihydroxyimidazolidine was recovered by filtration (0.98 g, 95% yield). This intermediate (0.34 g, 1.2 mmol) was dissolved in dichloromethane (200 ml) and vigorously stirred during 20 minutes with an aqueous solution (150 ml) of $NaIO_4$ (0.39 g, 1.8 mmol). The product was extracted with dichloromethane, the organic phase being dried over $MgSO_4$ and reduced to a minimum volume. Addition of *n*-hexane caused precipitation of the desired *o*-NITBAH radical (0.25 g, 75%). Mp 106–107 °C. Monocrystals were obtained by diffusion of hexane into a concentrated chloroform solution of the radical. UV–VIS λ_{max}/nm (ε/M^{-1} cm^{-1}) 222 (12559), 279 (7617), 296 (7670), 359 (5668), 370 (6357), 551 (879). IR (ν/cm^{-1}) 2996, 1705 (COOH), 1584, 1483, 1428, 1346 (NO), 1270, 1170, 1130, 755 (Found: C, 60.48; H, 6.02; N, 10.05. Calc. For $C_{14}H_{17}N_2O_4$ ($M_r=277.302$): C, 60.64; H, 6.18; N, 10.10%).

Crystallographic analysis†

Single crystals were isolated from a cluster of crystals and mounted on a rotation-free goniometer head. Systematic searches in reciprocal spaces using a Philips PW1100/16 automatic diffractometer with CuKα graphite monochromated radiation for *p*-IMBAH and a Nonius CAD4-F machine with MoKα graphite monochromated radiation for *m*-IMBAH and *o*-IMBAH showed that crystals of *m*-IMBAH and *p*-IMBAH belong to the monoclinic space group $P2_1/n$ and *o*-NITBAH to the monoclinic space group *Cc* or *C*2/*c*. Quantitative data were obtained at room temperature for *m*-IMBAH and *o*-NITBAH and at −100 °C for *p*-IMBAH. Selected experimental parameters are given in Table 4. The resulting data-sets were transfered to a DEC Alpha work station and subsequent calculations were made with the Nonius OpenMoleN package.[27] Three standard reflections measured every hour during the entire data collection period showed no significant trend. The raw data were converted to intensities and corrected for Lorentz and polarization factors. For *o*-NITBAH absorption corrections were derived from the y scans of 4 reflections.

The structures were solved using direct methods. For *o*-NITBAH, no solution could be found in space group *C*2/*c* and therefore space group *Cc* was used. After refinement of the heavy atoms, difference-Fourier maps revealed maxima of residual electronic density close to the positions expected for hydrogen atoms; they were introduced into structure-factor calculations by their computed coordinates (C–H = 0.95 Å) and isotropic temperature factors such as $B(H)=1.3$ *Beqv*(C) Å^2 but not refined (full matrix least-squares refinements; $\sigma^2(F^2)=\sigma^2_{counts}+(pI)^2$). The absolute structure of *o*-NITBAH was determined refining Flack's x parameter. Final difference maps revealed no significant maxima. The scattering factor coefficients and anomalous dispersion coefficients, respectively, were taken from references 28(*a*) and 28(*b*).

Other instrumentation

The EPR measurements were made at room temperature with an X-band (microwave frequency: *ca.* 9.8 GHz) spectrometer (Bruker ESR300) equipped with a rectangular TE 102 cavity. The static field was measured with an NMR Gaussmeter (Bruker ER035) while the microwave frequency was measured with a frequency meter (HP-5350 B), thus allowing for very accurate determination of the *g* factor, *i.e.* up to the fifth digit. The various parameters for the spectrometer (*e.g.* the amplitude of the modulation field and the microwave power), were controlled so as to avoid spurious signal distortions. Solutions were degassed with N_2 before recording the EPR spectra. The studies of the angular dependence of the EPR response of the single crystals were done with the aid of a one-axis goniometer (Bruker—ER218G1).

UV–VIS spectra: Unikon 933 (Kontron Instruments) spectrophotometer. FT-IR spectra: Bruker IFS 25 spectrometer; KBr pellets. Fast-atom bombardment (FAB, positive mode) ZAB-HF-VG-Analytical apparatus in a *m*-nitrobenzyl alcohol (*m*-NBA) matrix.

Acknowledgements

The authors are pleased to acknowledge continued technical assistance from Richard Poinsot of the Institut de Physique et de Chimie des Matériaux de Strasbourg (IPCMS), for the magnetic measurements and also Dr Marc Drillon for helpful discussions. This work was partially supported by the CNRS, the Engineer School of Chemistry (ECPM), and by the Human Capital and Mobility Program of E.U. (Network: 'Magnetic Molecular Materials', No ERBCHRXCT 920080).

References

1 J. S. Miller, A. J. Epstein and W. M. Reiff, *Chem. Rev.*, 1988, **88**, 201; *Acc. Chem. Res.*, 1988, **21**, 114; O. Kahn, *Molecular*

†Full crystallographic details, excluding structure factor tables, have been deposited at the Cambridge Crystallographic Data Centre (CCDC). For details of the deposition scheme, see 'Information for Authors', *J. Mater. Chem.*, available *via* the RSC web page (http://www.rsc.org/authors). Any request to the CCDC for this material should quote the full literature citation and the reference number 1145/136. See http://www.rsc.org/suppdata/jm/1999/875/ for crystallographic files in .cif format.

Magnetism, VCH, New York, 1993; *Molecular Magnetism: From Molecular Assemblies to the Devices*, ed. E. Coronado, P. Delhaès, D. Gatteschi and J. S. Miller, Nato ASI Series, Vol. 321, Kluwer Academic Publishers, Dordrecht, 1996.
2 M. Kinoshita, P. Turek, M. Tamura, K. Nozawa, D. Shiomi, Y. Nakazawa, M. Ishikawa, M. Takahashi, K. Awaga, T. Inabe and Y. Maruyama, *Chem. Lett*., 1991, 1225.
3 R. Chiarelli, M. A. Novak, A. Rassat and J. L. Tholence, *Nature*, 1993, **363**, 147.
4 T. Nogami, T. Ishida, H. Tsuboi, H. Yoshikawa, H. Yamamoto, M. Yasui, F. Iwasaki, H. Iwamura, N. Takeda and M. Ishikawa, *Chem. Lett*., 1995, 635 and references cited therein.
5 G. R. Desiraju, *Acc. Chem. Res*., 1991, **24**, 290; *Angew. Chem.*, *Int. Ed. Engl*., 1995, **34**, 2311, and references cited therein.
6 B. N. Figgis, E. S. Kucharski and M. Vrtis, *J. Am. Chem. Soc*., 1993, **115**, 176 and references cited therein.
7 E. Hernàndez, M. Mas, E. Molins, C. Rovira and J. Veciana, *Angew. Chem.*, *Int. Ed. Engl*., 1993, **32**, 882.
8 T. Sugawara, M. M. Matsushita, A. Izuoka, N. Wada, N. Takeda and M. Ishikawa, *J. Chem. Soc.*, *Chem. Commun*., 1994, 1723.
9 F. M. Romero, R. Ziessel, M. Drillon, J.-L. Tholence, C. Paulsen, N. Kyritsakas and J. Fischer, *Adv. Mater*., 1996, **12**, 826.
10 Y. Pontillon, E. Ressouche, F. Romero, J. Schweizer and R. Ziessel, *Physica B*, 1997, 235.
11 M. M. Matsushita, A. Izuoka, T. Sugawara, T. Kobayashi, N. Wada, N. Takeda and M. Ishikawa, *J. Am. Chem. Soc*., 1997, **119**, 4369.
12 K. Inoue and H. Iwamura, *Chem. Phys. Lett.*, 1993, **207**, 551.
13 N. C. Schiødt, F. Fabrizi de Biani, A. Caneschi and D. Gatteschi, *Inorg. Chim. Acta*, 1996, **248**, 139.
14 M. Drillon, C. Hornick, V. Laget, P. Rabu, F. M. Romero, S. Rouba, G. Ulrich and R. Ziessel, *Mol. Cryst. Liq. Cryst*., 1995, **273**, 125.
15 V. Laget, C. Hornick, P. Rabu, M. Drillon, P. Turek and R. Ziessel, *Adv. Mater*., 1998, **10**, 1024.
16 T. Akaike, M. Yoshida, Y. Miyamoto, K. Sato, M. Kohno, K. Sasamoto, K. Miyazaki, S. Veda and H. Maeda, *Biochemistry*, 1993, **32**, 827.
17 M. Yoshida, T. Akaike, Y. Wada, K. Sato, K. Ikeda, S. Veda and H. Maeda, *Biochem. Biophys. Res. Commun*., 1994, **202**, 923.
18 S. Nishibayashi, M. Asanuma, M. Kohno, M. Goimez-Vargas and N. Ogawa, *J. Neurochem*., 1996, **67**, 2208.
19 R. Tsunoda, K. Okumura, H. Ishizaka, T. Matsunaga, T. Tabushi, H. Yasue, T. Akaike, K. Sato and H. Maeda, *Eur. J. Pharmacol*., 1994, **262**, 55.
20 E. F. Ullman, J. H. Osiecki, D. G. B. Boocock and R. Darcy, *J. Am. Chem. Soc*., 1972, **94**, 7049.
21 M. Lamchen and T. W. Mittag, *J. Chem. Soc. C*, 1966, 2300.
22 J. Cirujeda, E. Hernàndez-Gasio, C. Rovira, J.-L. Stanger, P. Turek and J. Veciana, *J. Mater. Chem.*, 1995, **5,** 243.
23 F. M. Romero, R. Ziessel, A. De Cian, J. Fischer and P. Turek, *New J. Chem*., 1996, **20**, 919.
24 A. Caneschi, P. Chiesi, L. David, F. Ferraro, D. Gatteschi and R. Sessoli, *Inorg. Chem.*, 1993, **32**, 1445.
25 (*a*) A. Bencini and D. Gatteschi, *EPR of exchange coupled systems*, Springer-Verlag, Berlin, 1990; (*b*) P. Turek, *Mol. Cryst. Liq. Cryst*., 1993, **233**, 191.
26 T. Otsuka, T. Okuno, K. Awaga and T. Inabe, *J. Mater. Chem*., 1998, **8**, 1157.
27 OpenMoleN, Interactive Structure Solution, Nonius B.V., Delft, The Netherlands, 1997.
28 (*a*) Table 2.2b; (*b*) Table 2.3.1, D. T. Cromer and J. T. Waber, *International Tables for X-ray Crystallography*, 1974, Vol. IV, The Kynoch Press, Birmingham.

Paper 8/08018F